# Supplementary Information

## Band-Gap Tunable Thiadiazolo[3,4-*g*]quinoxaline Derivatives as Non-Fullerene Acceptors for Organic Photovoltaic Cells Processed from Low Toxic Ethanol/Anisole Mixtures

Cristiana Costa,[a,b] Joana Farinhas,[a] Mariana F.G. Velho,[a,c] João Avó,[d] Manuel Matos,[a,e] Adelino Galvão,[b] Ana Charas[a]

[a.] *Instituto de Telecomunicações, Instituto Superior Técnico, Av. Rovisco Pais 1, P-1049-001, Lisboa, Portugal. *Email:ana.charas@lx.it.pt*
[b.] *Centro de Química Estrutural, Instituto Superior Técnico, Universidade de Lisboa, Av Rovisco Pais, 1049-001 Lisboa, Portugal. *Email: adelino@tecnico.ulisboa.pt*
[c.] *$C^2TN$, Centro de Ciências e Tecnologias Nucleares, Instituto Superior Técnico, Universidade de Lisboa, E.N. 10, 2695-066, Bobadela LRS, Portugal.*
[d.] *CQFM-IN and IBB-Institute for Bioengineering and Biosciences, Instituto Superior Técnico, University of Lisbon, Lisboa, Portugal.*
[e.] *Departamento de Engenharia, Química, Instituto Superior de Engenharia de Lisboa, Lisboa, Portugal.*

## Contents

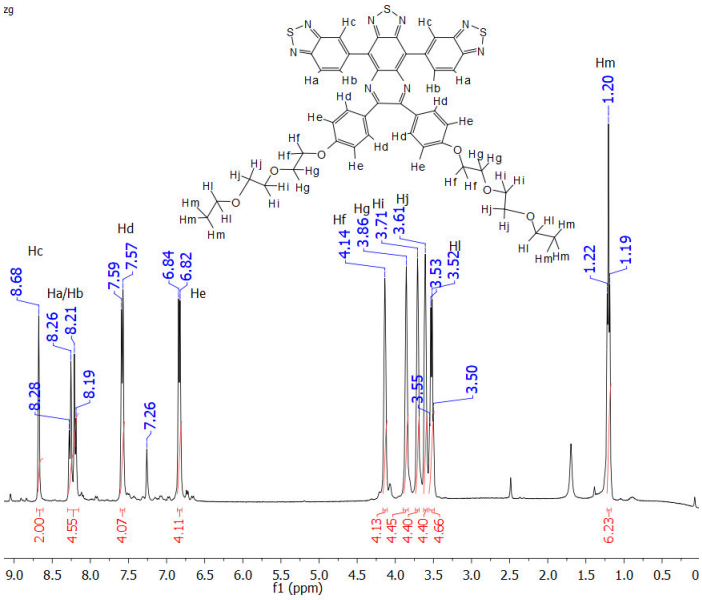


**Fig. S1** $^{1}$H-NMR (400 MHz) spectrum of TQBT in $CDCl_3$.

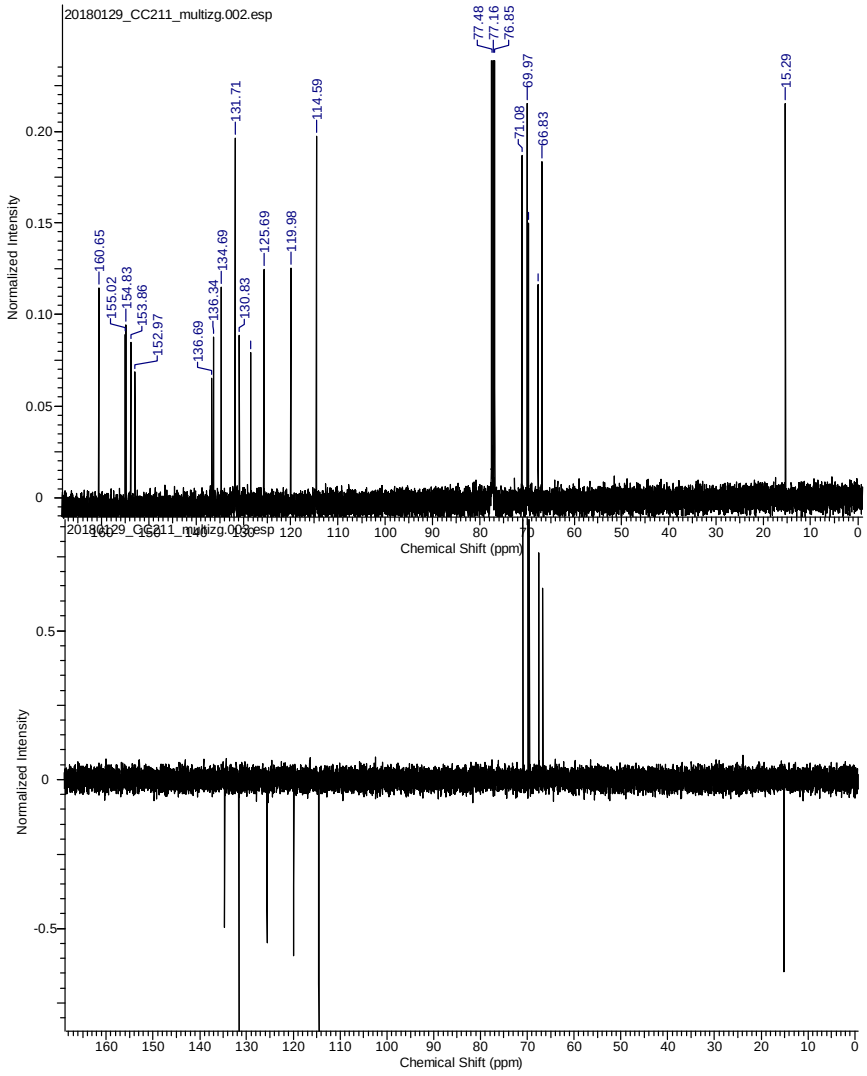


**Fig. S2** $^{13}$C (100 MHz) (top) and DEPT 135 (CH and *$CH_3$'s* appearing negative and $CH_2$'s appearing positive) NMR spectrum (bottom) of TQBT in $CDCl_3$.

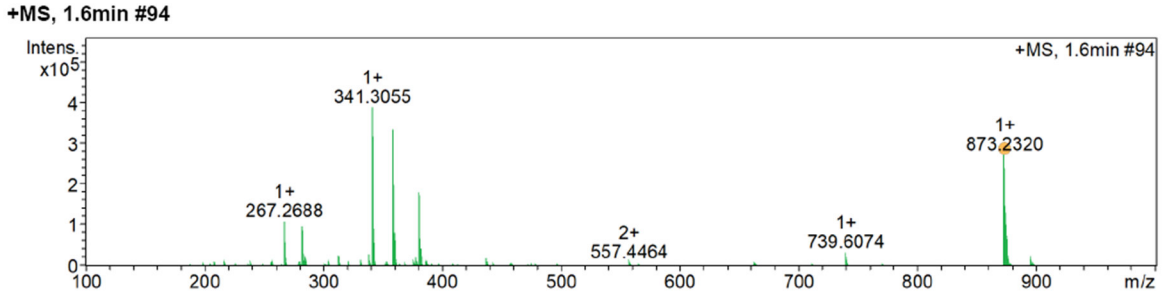


**Fig. S3** HRMS spectrum of TQBT.

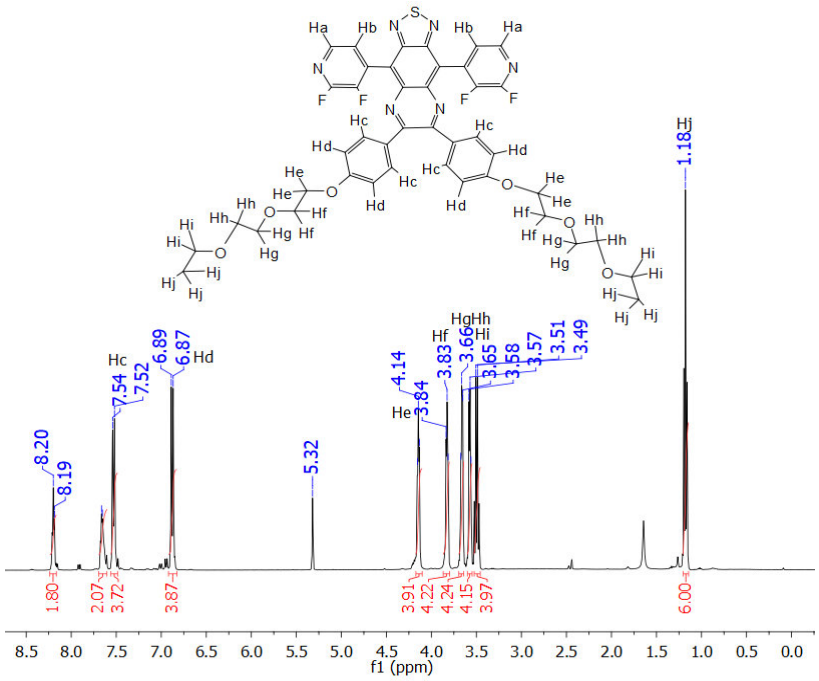


**Fig. S4** $^{1}$H-NMR (400 MHz) spectrum of TQFP in $CD_2Cl_2$.

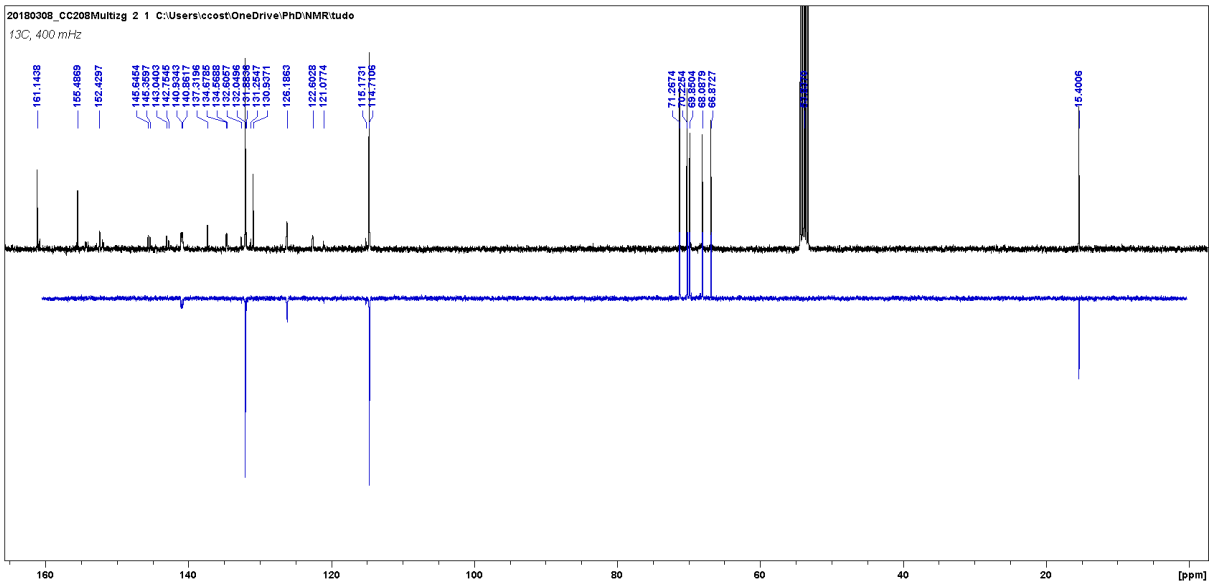


**Fig. S5** $^{13}$C (100 MHz) (top) and DEPT 135 (CH and *$CH_3$'s* appearing negative and $CH_2$'s appearing positive) NMR spectrum (bottom) of TQFP in $CD_2Cl_2$.

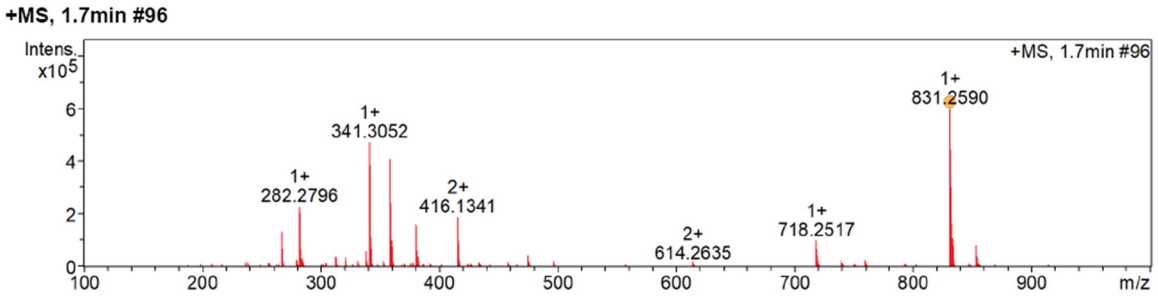


**Fig. S6** HRMS spectrum of TQFP.

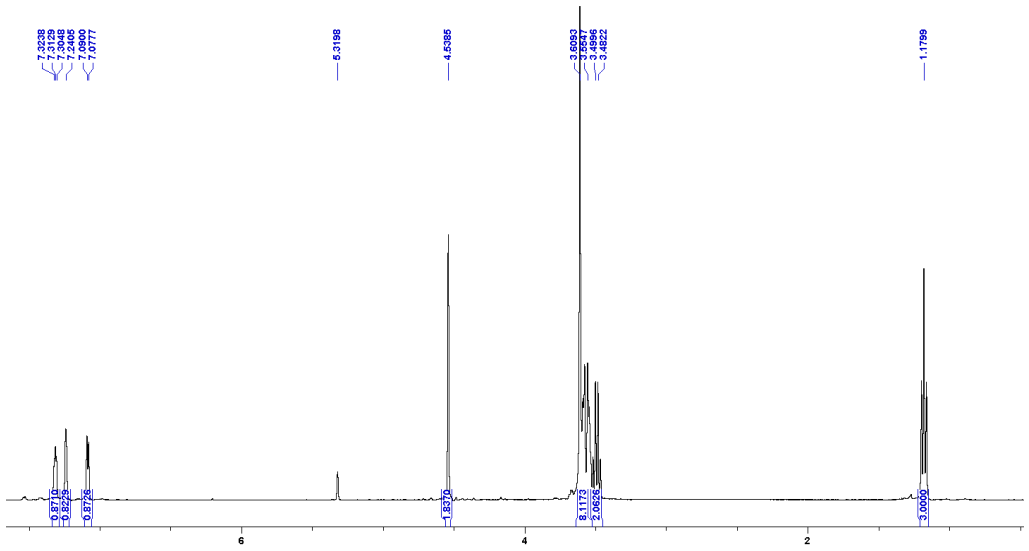

**Fig. S7** $^{1}$H-NMR (400 MHz) spectrum of 3-{[2-(2-ethoxyethoxy)ethoxy]methyl}thiophene (2) in $CD_2Cl_2$.

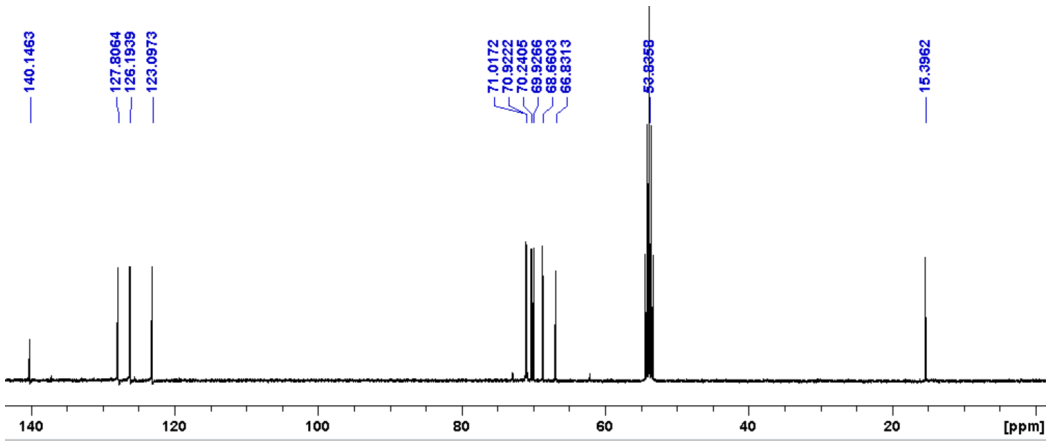


**Fig. S8** $^{13}$C-NMR (75 MHz) spectrum of 3-{[2-(2-ethoxyethoxy)ethoxy]methyl}thiophene (2) in $CD_2Cl_2$.

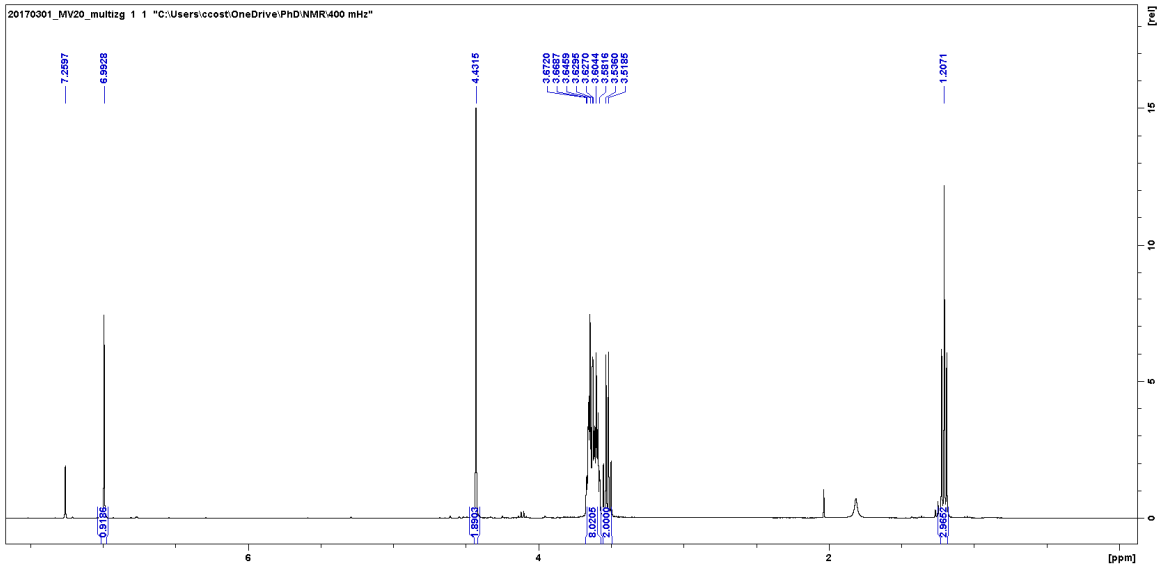


**Fig. S9** $^{1}$H-NMR (400 MHz) spectrum of 2,5-dibromo-3-{[2-(2-ethoxyethoxy)ethoxy]methyl} thiophene (3) in $CDCl_3$.

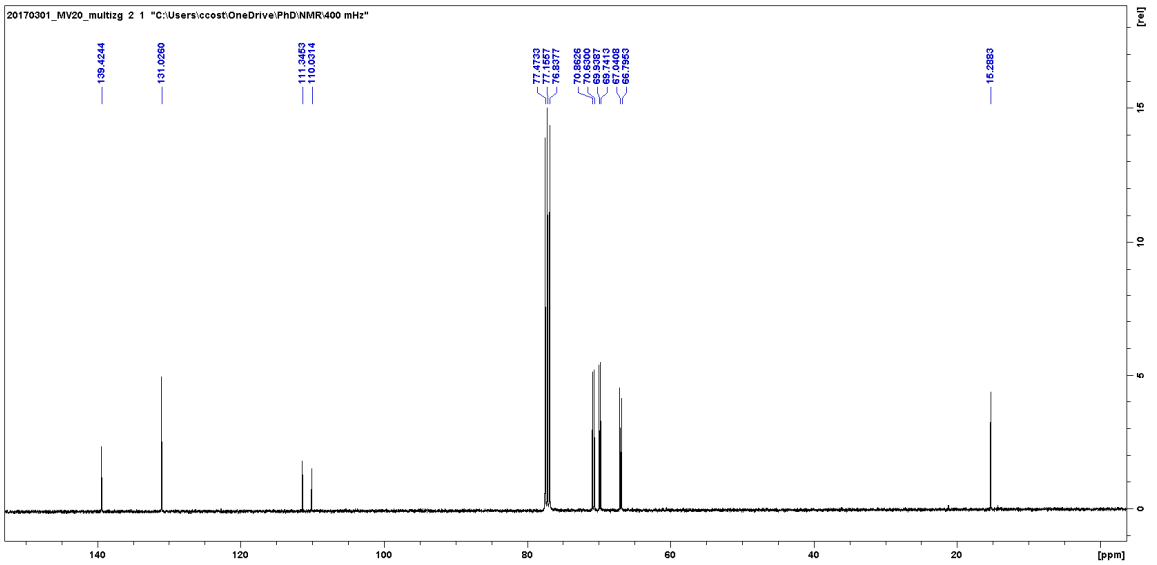


**Fig. S10** $^{13}$C-NMR (75 MHz) spectrum of 2,5-dibromo-3-{[2-(2-ethoxyethoxy)ethoxy]methyl}thiophene (3) in $CDCl_3$.

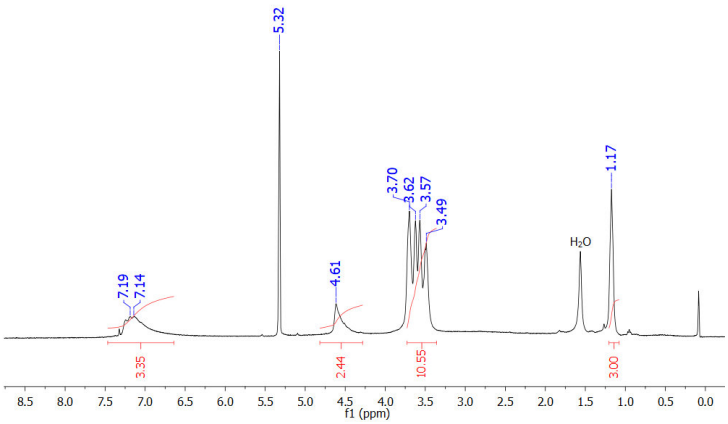


**Fig. S11** $^{1}$H-NMR (400 MHz) spectrum of POEGT in $CD_2Cl_2$ and signal ratios.

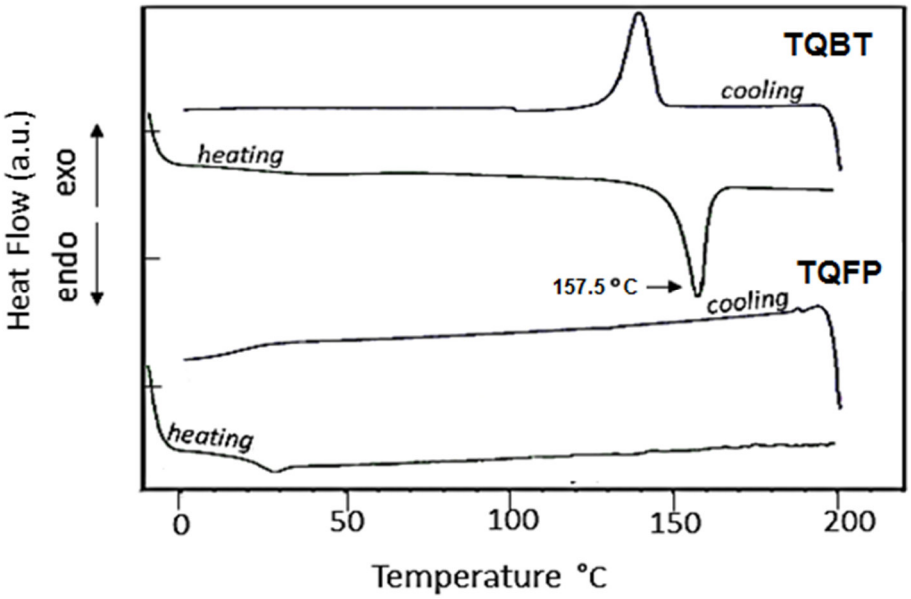


**Fig. S12** Differential Scanning Calorometry (DSC) thermograms of TQBT and TQFP (Scan rate = 10 °C/min).

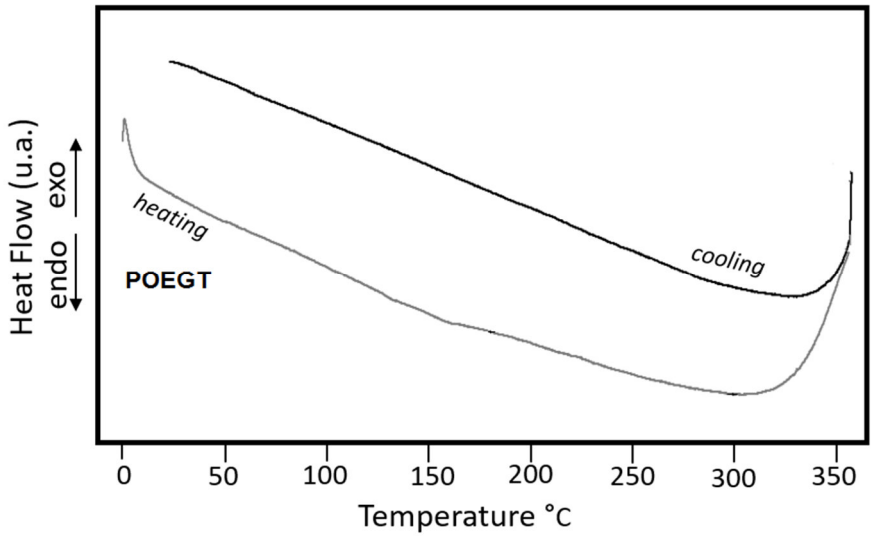


**Fig. S13** Differential Scanning Calorometry (DSC) thermograms of POEGT (Scan rate = 10 °C/min).

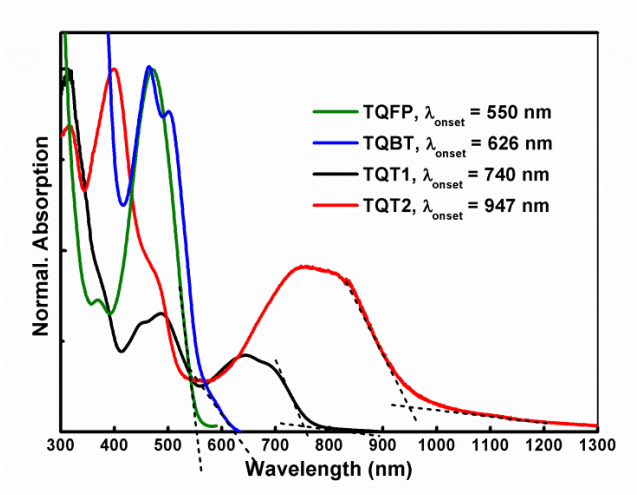


**Fig. S14.** UV-Vis absorption spectra of TQFP, TQBT, TQT1 and TQT2 in films showing the onset of the lowest energy absorption bands.

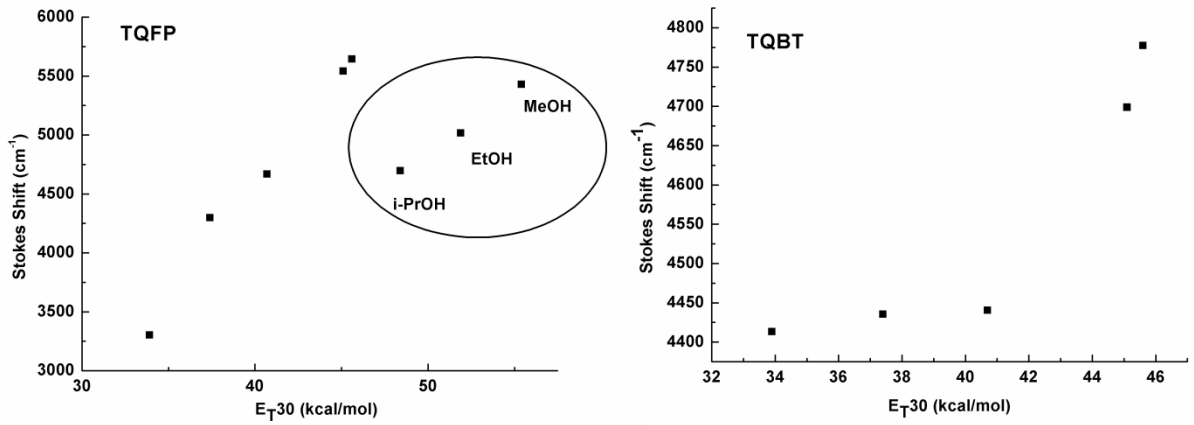


**Fig. S15** Stokes shifts as a function of the solvent polarity parameter Et30 for TQFP and TQBT.

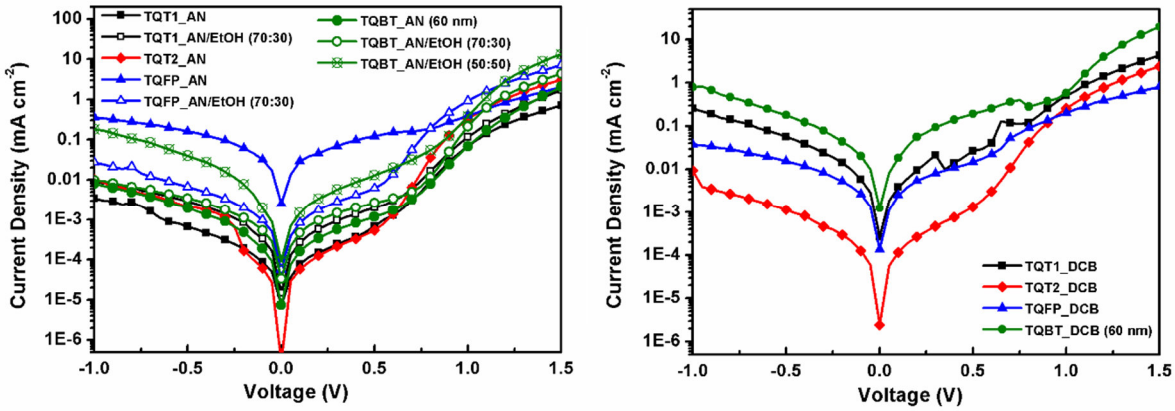


**Fig. S16** Dark J-V curves for the OSCs prepared from 1:1 (D:A) blends in various solvents.

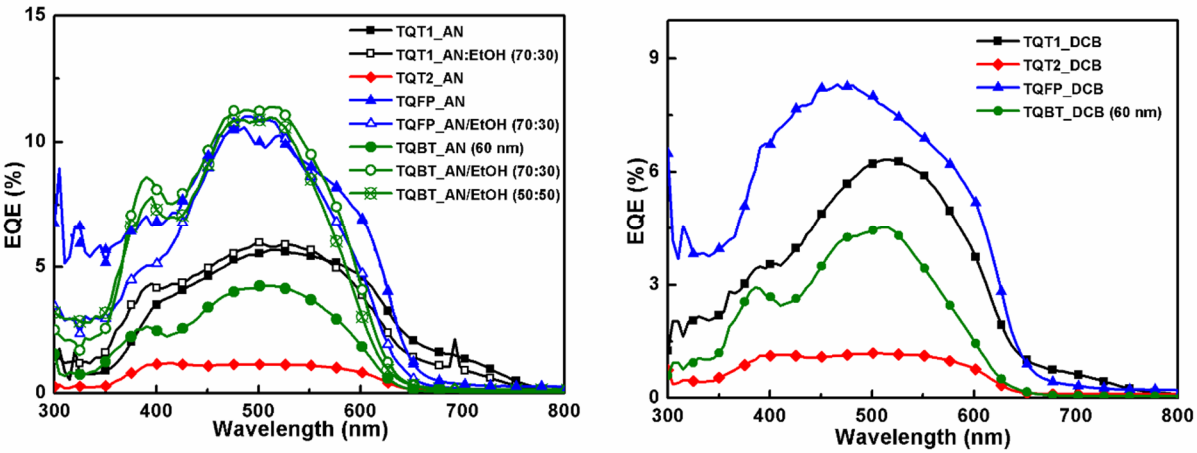


**Fig. S17** EQE spectra for the OSCs prepared from 1:1 (D:A) blends in various solvents.

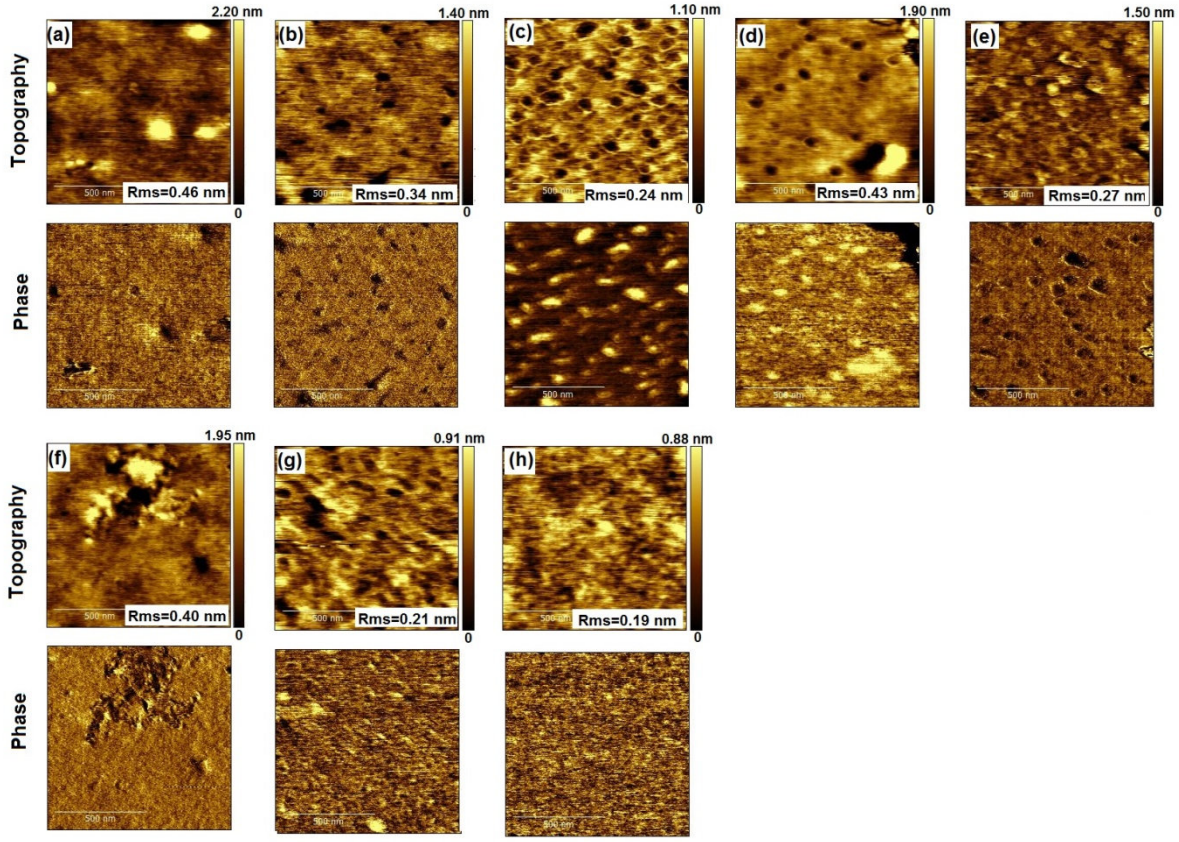


**Fig. S18** AFM topography (upper) and phase (down) images of blend films of: POEGT:TQT1 processed from DCB (a), Anisole (AN) (b), AN/EtOH (70:30) (c); POEGT:TQT2 processed from DCB (d), AN (e); POEGT:TQFP processed from DCB (f), AN (g) and AN/EtOH (70:30) (h).

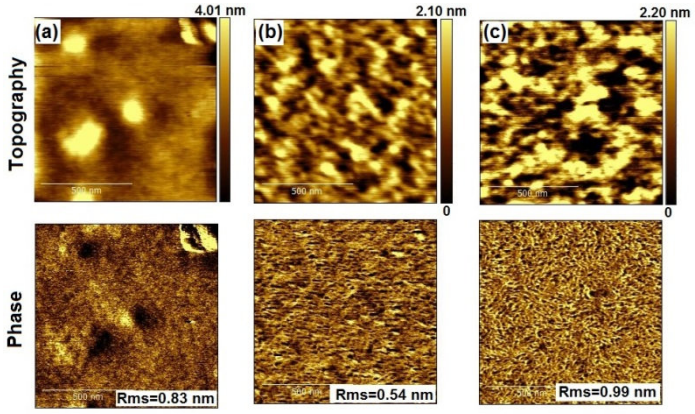


**Fig. S19** AFM topography and phase images of active layers composed of POEGT:TQFP 1:2 ratio (a); POEGT:TQBT 2:1 ratio (b); and POEGT:TQBT 1:2 ratio (c).

**Table S1** Performance parameters of the OSCs prepared with 1:2 or 2:1 (D:A) blends.

| Active layer (AN/EtOH 70:30) | D:A ratio | $J_{SC}$ (mA/cm$^2$) | $V_{OC}$ (V) | FF | PCE (%) best/ave[a] | AL Thickn (nm) |
|---|---|---|---|---|---|---|
| **POEGT:TQFP** | 1:2 | -1.19 | 0.70 | 0.33 | 0.27/0.20 | 70 |
| **POEGT:TQBT** | 2:1 | -0.70 | 0.84 | 0.26 | 0.16/0.15 | 80 |
| | 1:2 | -1.27 | 0.86 | 0.31 | 0.34/0.31 | 85 |

[a] Best values followed by the averages calculated from at least 8 devices.